2023-01

Artificial reefs built by 3D printing: Systematisation in the design, material selection and fabrication

Yoris-Nobile, AI

10.1016/j.conbuildmat.2022.129766
Construction and Building Materials
Elsevier BV

Construction and Building Materials 362 (2023) 129766

Contents lists available at ScienceDirect

Construction and Building Materials

journal homepage: www.elsevier.com/locate/conbuildmat

Artificial reefs built by 3D printing: Systematisation in the design, material selection and fabrication

Adrian I. Yoris-Nobile [a], Carlos J. Slebi-Acevedo [b], Esther Lizasoain-Arteaga [c], Irune Indacoechea-Vega [a], Elena Blanco-Fernandez [a,*], Daniel Castro-Fresno [a], Alejandro Alonso-Estebanez [a], Sara Alonso-Cañon [a], Carlos Real-Gutierrez [a], Fouad Boukhelf [d], Mohamed Boutouil [d], Nassim Sebaibi [d], Alice Hall [e], Sam Greenhill [f], Roger Herbert [f], Richard Stafford [f], Bianca Reis [g,h], Pieter van der Linden [g,h], Oscar Babé Gómez [g,h], Hugo Sainz Meyer [g,h], João N. Franco [g,h,i], Emanuel Almada [g,h,j], Maria Teresa Borges [g,h], Isabel Sousa-Pinto [g,h], Miriam Tuaty-Guerra [h,l], Jorge Lobo-Arteaga [k,l]

[a] GITECO Research Group, Universidad de Cantabria, Avda. Los Castros 44, 39005 Santander, Spain
[b] Civil and Environmental Engineering Department, Escuela Colombiana de Ingeniería Julio Garavito, Bogotá Colombia
[c] TECNALIA, Basque Research and Technology Alliance (BRTA), Spain
[d] ComUE NU, Laboratoire de Recherche ESITC Caen, 1 Rue Pierre et Marie Curie, 14610 Epron, France
[e] School of Biological and Marine Sciences, Marine Institute, Plymouth University, Drake Circus, Plymouth PL4 8AA, UK
[f] Dept. Life and Environmental Sciences, Bournemouth University, BH12 5BB, UK
[g] Faculdade de Ciências, Universidade do Porto, Rua do Campo Alegre s/n, 4150-181 Porto, Portugal
[h] CIIMAR, Centro Interdisciplinar de Investigação Marinha e Ambiental, Terminal de Cruzeiros do Porto de Leixões, Av. General Norton de Matos s/n, 4450-208 Matosinhos, Portugal
[i] MARE - Marine and Environmental Sciences Centre, ESTM, Politécnico de Leiria, 2520-620 Peniche, Portugal
[j] MARE - Marine and Environmental Sciences Centre, Quinta do Lorde Marina, Sitio da Piedade, 9200-044 Madeira, Portugal
[k] MARE - Marine and Environmental Sciences Centre, Universidade Nova de Lisboa, Campus de Caparica, 2829-516 Caparica, Portugal
[l] Instituto Português do Mar e da Atmosfera, I.P.M.A., Divisão de Oceanografia e Ambiente Marinho, Rua Alfredo Magalhães Ramalho 6, 1495-165 Algés, Portugal

ARTICLE INFO

Keywords:
Concrete 3D printing
Life Cycle Assessment (LCA)
Numerical simulations
Multi-Criteria Decision-Making Analysis (MCDM)
Artificial reefs (ARs)

ABSTRACT

The recovery of degraded marine coasts and the improvement of natural habitats are current issues of vital importance for the development of life, both marine and terrestrial. In this sense, the immersion of artificial reefs (ARs) in the marine environment is a way to stimulate the recovery of these damaged ecosystems. But it is necessary to have a multidisciplinary approach that analyses the materials, designs and construction process of artificial reefs in order to understand their true impact on the environment. For this reason, this paper presents the manufacture of artificial reefs by 3D printing, proposing designs with a combination of prismatic and random shapes, with different external overhangs as well as inner holes. For the definition of the artificial reef designs, criteria provided by marine biologists and the results obtained from a numerical simulation with ANSYS were taken into account, with which the stability of the artificial reefs on the seabed was analysed. Three dosages of cement mortars and three dosages of geopolymer mortars were studied as impression materials. The studies included determination of the rheological properties of the mortars, to define the printability, determination of the cost of the materials used, and determination of the mechanical strength and biological receptivity in prismatic specimens that were immersed in the sea for 3 months. To evaluate the environmental impact of the materials used in the production of the mortars, a Life Cycle Assessment (LCA) was carried out. In order to choose the mortars that encompassed the best properties studied, Multi-Criteria Decision Making (MCDM) was applied and the two best mortars were used for the manufacture of the artificial reefs. Finally, the advantages and disadvantages of the 3D printing process used were analysed. The results of the studies carried out in this research show that cement mortars have better characteristics for artificial reef applications using 3D printing, and that the technique applied for the manufacture of the artificial reefs allowed the digital models to be faithfully reproduced.

* Corresponding author.
E-mail address: elena.blanco@unican.es (E. Blanco-Fernandez).

https://doi.org/10.1016/j.conbuildmat.2022.129766
Received 29 August 2022; Received in revised form 21 October 2022; Accepted 13 November 2022
Available online 21 November 2022

1. Introduction

The use of ARs is a technique that helps the recovery of environmentally degraded coastal areas and complements the existing natural ones, creating a favourable habitat for the development of marine life [1,2], even emulating the capacity of natural reefs to support marine life [3]. They also have social and economic benefits for local fishing communities [4,5], are used to stabilise marine coasts [6], protect the seabed from trawling methods [6], and promote diving tourism [2], among others. The immersion of ARs in marine coasts has been applied for years in various parts of the world using different objects, such as used cars, wrecks, tyres, stone or concrete blocks, and more recently, pre-designed elements with shapes that tend to reproduce natural environments [6–10]. Some research suggests that the use of concrete as a manufacturing material for artificial reefs, together with high surface roughness, allows for more efficient biological colonisation [3,10]. The external shapes of ARs, the sizes and shapes of the holes, the surface roughness or texture, the type of material used in the fabrication, among other characteristics, have a direct relationship with the attraction or development of marine life in a particular area [11–14].

Additive manufacturing or 3D printing can play a key role in the manufacture of ARs, as it allows the creation of specifically designed models, giving the possibility to optimise their shapes and textures to attract as much marine life as possible, i.e. to simulate natural environments [15–17]. The fabrication of ARs by 3D printing is not a new topic, there are several initiatives and projects that propose different shape designs [18–21]. However, information regarding design, materials used and characterisation of the deployment site is still very scarce [22]. Furthermore, systematisation of the monitoring method after deployment together with finding correlations between shapes and/or materials with bio-colonisation performance is still insufficient [22].

3D printing is a technology that has been progressively introduced in the construction industry. In particular, technology based on Extruded Material Systems (EMS) presents greater versatility than that based on Powder Based Systems (PBS), helping to achieve larger three-dimensional elements [23]. Another advantage of EMS vs PBS systems is that in the first one, mortar is previously mixed, thus, guaranteeing the hydration of the cement. Contrary, in PBS systems water drops are sprayed over a lay of dry mortar without mixing it afterwards. This implies that an adequate cement hydration is not always guaranteed, which might lead to a strength reduction. Other advantages of additive manufacturing include eliminating the use of formwork, reducing material waste and optimising resources [24]. However, the level of complexity of EMS concrete printers is often limited to the construction of vertical walls on a random flat layout [25]. For this reason, a hybrid printing system combining EMS and PBS methodologies was proposed to fabricate the ARs in this work, with a high level of complexity of ARs' designs.

The use of sustainable materials in the field of construction is nowadays considered a relevant requirement, becoming, in the case of artificial reefs, even more important due to their remarkable environmental character. Some lines of research point to the use of alternative or low clinker content binders, while others propose the replacement of natural aggregates with recycled aggregates or industrial by-products [13,26]. Some research indicates the feasibility and benefits of using recycled or alternative materials in the manufacture of ARs. Materials such as fluorogypsum, steel and blast furnace slag concrete, sulphoaluminate cement, among others, have been successfully used for ARs [12,26,27]. A reference in this field is the company EcoConcrete, which is dedicated to the manufacture of components for different uses in the marine environment, with a focus on sustainability in the materials used and contributing to the attraction of marine biodiversity [28]. As impression material, low clinker cement mortars, geopolymer mortars and recycled aggregates in both cases (crushed glass and seashells) are studied in this paper.

The reefs designed in this work were agreed with biologists, who provided their experience in the field to define the shapes that were considered most suitable for attracting marine life. These designs were then subjected to an analysis of structural integrity and stability on the seabed, so that they would not be broken or drifted by the action of ocean currents and waves.

The use of DoE (Design of Experiments) to define the potential shapes of ARs, the combination of PBS and EMS 3D printing process and the MCDMA to select the best materials to build ARs taking into account cost, printability, LCA and bioreceptivity are the major novel contributions of this paper.

2. Material and methodology

2.1. Material and characterisation

For the production of ARs, the use of mortars with low environmental impact was sought, so cement-based mortars with low clinker content and geopolymer-based mortar were analysed, as several authors point out that the production of geopolymers is more sustainable than that of cement-based materials [29–33]. The main components of the cement mortars were: cement type III/B 32,5N-SR (31 %: clinker, rest: blast furnace slag), fly ash [34]; seashell sand, crushed glass sand [35,36] and limestone sand. Particle size was 0–1 mm for seashell sand, 0–0.3 mm for crushed glass and 0–3 mm for limestone sand. Geopolymer mortars were composed of fly ash, sodium hydroxide (NaOH) and the same aggregates employed in the cement mortars. In Table 1 the dosages of the mortars employed in the analysis are indicated. Details of the material characterisation and processing of the mortars are given in [37].

The characteristics of the mortars analysed in this work correspond to: biological receptivity, compressive strength, printability and cost of the mixtures. Both biological receptivity and compressive strength were determined in prismatic specimens of 4 × 4 × 16 cm, which were obtained by cutting samples from 3D printed slabs. The mechanical resistance was obtained according to test standard EN 196-1 [38], while bioreceptivity was determined with dry weight (105 °C) of the biomass (flora and fauna) adhered to the specimens. The 3D printed plate fabrication, the specimen cutting, and the determination of biological

Table 1
Dosages of cement and geopolymer mortars.

Cement mortars [kg/m^3]				Geopolymer mortars [kg/m^3]			
Materials	CL	CS	CG	Materials	GL	GS	GG
Cem. III/B	521.6	493.8	504.8	Fly Ash	592.5	523.3	576.7
Water	278.5	311.9	287.8	NaOH [14 M]	267.0	305.0	276.0
Fly Ash	260.8	246.9	252.4	Water	26.7	30.5	27.6
Kaolin	21.7	20.6	21.0	N.S.	29.6	26.2	28.8
S.P.	3.7	4.4	3.0	M.S.	59.2	52.3	57.7
Limestone [0–3]	1043.2	493.8	504.8	Limestone [0–3]	1184.9	523.3	807.4
Seashells	–	493.8	–	Seashells	–	523.3	–
Glass [0–0.3]	–	–	504.8	Glass [0–0.3]	–	–	346.0

Note: C: cement; G: geopolymer; L: limestone sand; S: shell sand; G: glass sand; SP: superplastifyer; NS:nanosilica; MS:microsilica.

Table 2
Cost of individual materials.

Material	Cem III/B	F.A.	Kaolin	S.P.	Limestone	N.S.	M.S.	NaOH
Cost (€/kg)	0.10	0.08	0.15	2.63	0.01	4.00	2.00	0.60

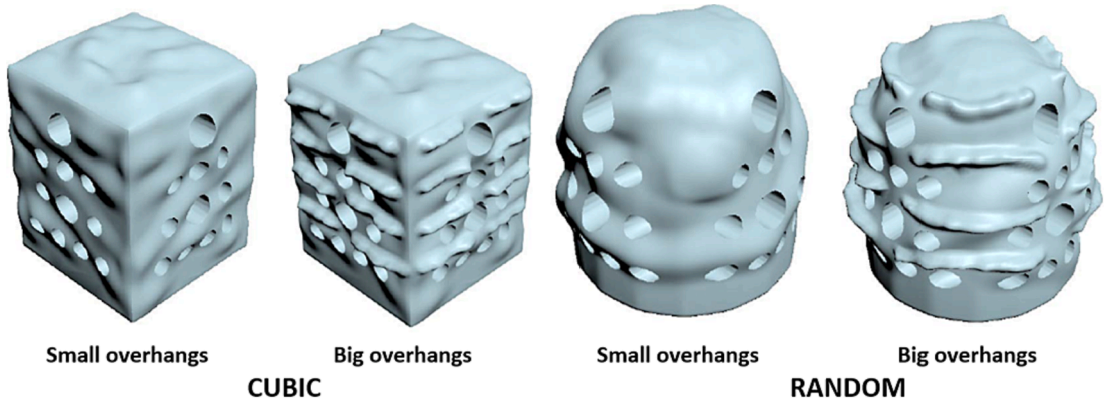

Fig. 1. Four models of the artificial reefs.

Fig. 2. Control block.

receptivity were carried out according to [39].

At 70 days of age, the specimens were submerged in different marine coasts of the Atlantic Ocean of United Kingdom (UK), France (FR), Spain (SP) and Portugal (PT). During this period, the specimens were kept in the air in laboratory environment, only exposed to water during the cutting period of the printed plates, which lasted approximately-one week. The results shown in this work correspond to 3 months of immersion. Once the specimens were removed from the sea and the biomass adhered to them was removed, the specimens were kept wrapped in plastic in a laboratory environment for one week, after which they were tested. Printability was classified from 1 to 3, in which 3 is very good; 2 is good and 1 is regular. On the other hand, costs of the mortars were determined based on the costs of their components (Table 2). Recycled aggregates were considered at no cost because they are industrial waste and water was also considered at no cost because it has a minimal value compared to the other materials. The methodology used for the determination of the rheological parameters and the material cost databases are given in [37].

2.2. Artificial reef design

With the aim to study with a systematic approach the influence of materials and shapes in the bio-colonisation of ARs, 9 different blocks have been designed and a total of 36 ARs (4 locations × 9 blocks) have been fabricated with a concrete 3D printer with the aim of carrying out a bio-colonisation campaign for a minimum of 2 years in four locations: Dinard Bay (FR), Poole Bay (UK), Porto (PT) and Santander (SP).

The nine blocks have been selected based on a DoE, where 4 shapes (Fig. 1) × 2 materials have been considered together with a ninth control block (Fig. 2). The 4 shapes are based on a combination of 2 external overall shapes (cubic, random) and also 2 external types of irregularities (big overhangs, small overhangs). Control block consists of a cubic solid block; nevertheless, in order to study the influence between textures, two vertical faces have a 3D printer finish (extruded filaments of mortar are exposed) while the other two have a flat finish, emulating a standard jetty concrete block. The top side has half of the surface with a 3D printing finish and the other half with a flat finish.

An identical pattern of holes has been defined for both the cubic model (Fig. 3) and random model (Fig. 4). The pattern consists of 4 rows of holes at each of the four vertical faces. From bottom to top, the first row has 4 holes of 80 mm diameter, second row 3 holes −2 laterals with 80 mm diameter and a central hole of 120 mm diameter-, third row has 3 holes of 80 mm diameter, and fourth row has 1 single whole of 120 mm diameter. Some of the holes are tunnels while others have no exit.

In order to simplify the printing process, reinforcement bars were not included. As it has been discussed in the numerical simulations sections (2.3 and 3.2), the ARs could stand the forces exerted by the water without the need of reinforcement bars. The use of fibers to reduce the section of the ARs was also discarded, because the maximum increment on flexural strength that fibers could supply would not be more than 30 % [40], which is considered still quite low to be contemplated as a substitute of rebars.

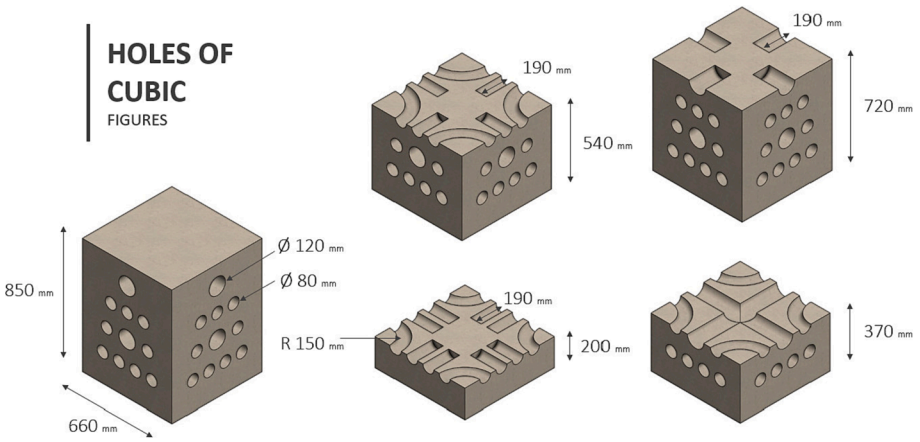

Fig. 3. Holes distribution for the cubic model.

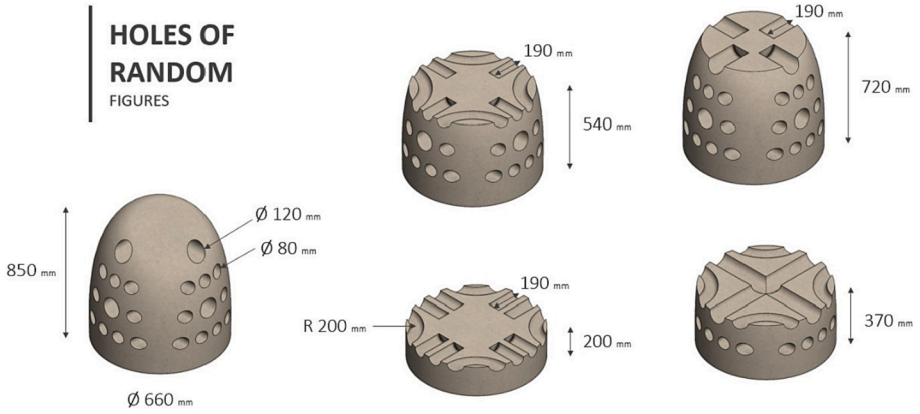

Fig. 4. Holes distribution for the random model.

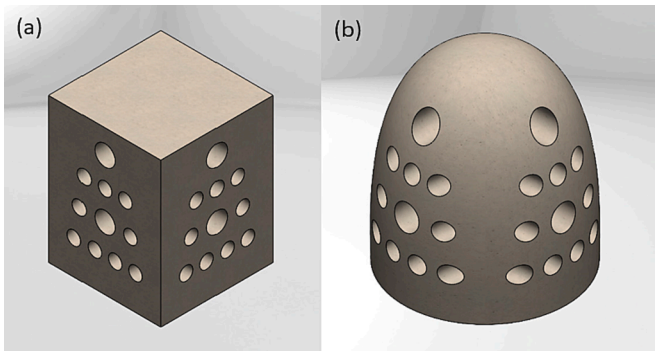

Fig. 5. The CAD geometries proposed for the cubic reef (a) and for the random reef (b).

2.3. Numerical simulation

Numerical simulation software ANSYS was used to develop the numerical models to analyse the reef structural behaviour. Specifically, the Computational Fluid Dynamic (CFD) code FLUENT was used for simulating the sea conditions and to obtain the sea forces acting on the reefs and the mechanical module was used to analyse the reefs' structural stability. Both geometries studied are shown in Fig. 5.

The mesh of finite volumes was built both for the fluid domain and for the ARs geometries in the CFD and structural analysis, respectively. Whereas the CFD code requires to mesh the fluid region, in the structural module it was only necessary to mesh the ARs geometry. In the CFD code, the meshes consisted of tetrahedral and hexahedral cells while for the structural analyses only tetrahedral cells were used. The fluid region closer to ARs surface is more densely meshed to capture properly the higher gradients in the flow variables due to a friction between the fluid and solid surfaces (Fig. 6). The maximum number of cells used in the mesh was around 0.7 million.

In the next step, the boundary conditions were set both for the dynamic fluid analysis and for the structural analysis. The dynamic fluid analysis was carried out before the structural analyses, as the sea forces acting on the artificial reef are imported from the CFD code into the structural module. The boundary condition set to solve the numerical model in FLUENT is shown in Fig. 7. The boundary conditions and actions were defined according to the most critical condition at ARs location for its stability and structural integrity, which were at Santander bay. The water inlet surface was defined as an inlet velocity of 2 m/s and the water outlet surface was defined as a relative pressure of 0 Pa. A wave height of 1.5 m and a length of 8 m was set along with a free surface level equal to 3 m, minimum sea depth recorded at location. The combination of maximum wave height and minimum sea depth are the worst conditions for the structural integrity of the artificial reef, although it is unlikely that they will actually occur simultaneously. The dimensions of domain of fluid are 35 m long, 11 m width and 5 m height. Potential biomass adherence has not been taken into account in the simulation of the ARs, since it is believed that its influence on the stresses should be quite low.

In the CFD model, an unsteady analysis, 120 s long with a time step of 0.01 s, was developed to estimate the oscillating forces acting on the ARs. The first 20 s were discarded for the calculation of forces due to numerical instabilities. The equation of conservation of mass and

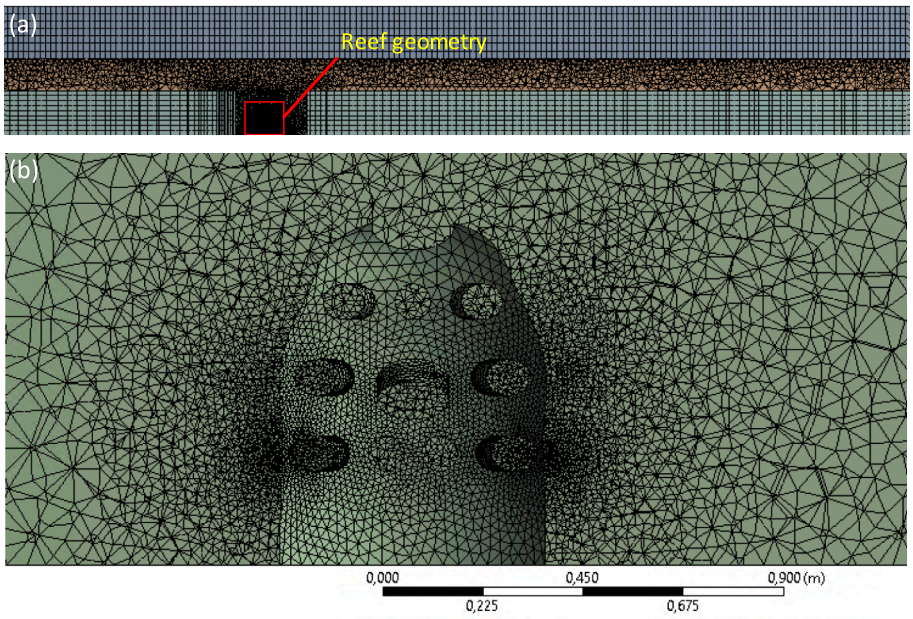

Fig. 6. Mesh for the fluid domain regions (a) and mesh built for the water regions (b) close to the reef geometry (random model).

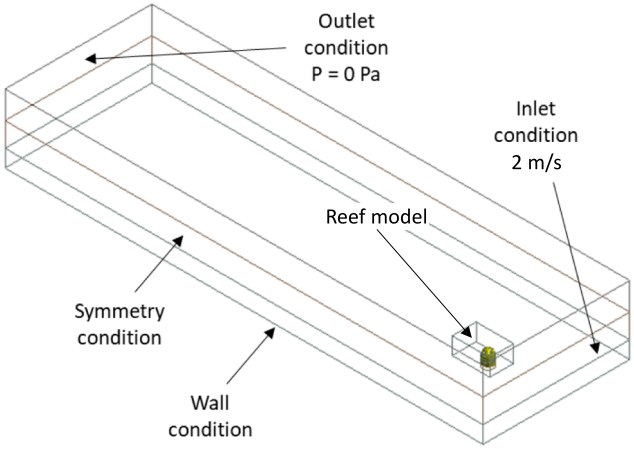

Fig. 7. Boundary condition set in the numerical setup.

momentum along with a viscous model and a multiphase model were solved by applying the Finite Volume Method. The turbulence model k-Ɛ [41–43] was selected to model the viscous behaviour of fluid and the Volume of Fluid (VOF) model was used to simulate the interaction between the two phases (air and water). Regarding the solution method, SIMPLEC scheme was applied for solving the pressure–velocity coupling and second order Upwind scheme was set as spatial discretisation method for the variables from the turbulence model [41]. In Fig. 8, the water volume fraction is presented by a snapshot in time around one of the artificial reef geometries.

2.4. Life Cycle Assessment (LCA)

To feed the MCDM analysis and select the best dosages, an LCA of the mortars listed in Table 1 was carried out, following the recommendations of ISO 14040:2006 [44] and 14044:2006 [45] standards. For the analysis, 1 t of mixture and 1 MPa was selected as functional unit; this is because the same amount by weight of different materials could have different strengths, i.e., one material with twice the strength of another could use half as much material as the other. The values of strength adopted were the averaged compressive strength of prismatic samples after 3 months immersion (Fig. 12). In the analysis, only the production stage was included within the system boundaries assuming that the other life-cycle stages would not significantly change.

The processes inventory information was collected mainly from GaBi V9.1 database for electricity, fossil fuel, cement, superplasticizer, water, micro-silica and sodium hydroxide production. As micro-silica is a by-product of the ferrosilicon alloys generation and GaBi process does not distinguish between co-products, an impact allocation was applied by considering the quantities and costs of each material [46]. Furthermore, other databases and literature were also checked to complete the inventory (Table 3).

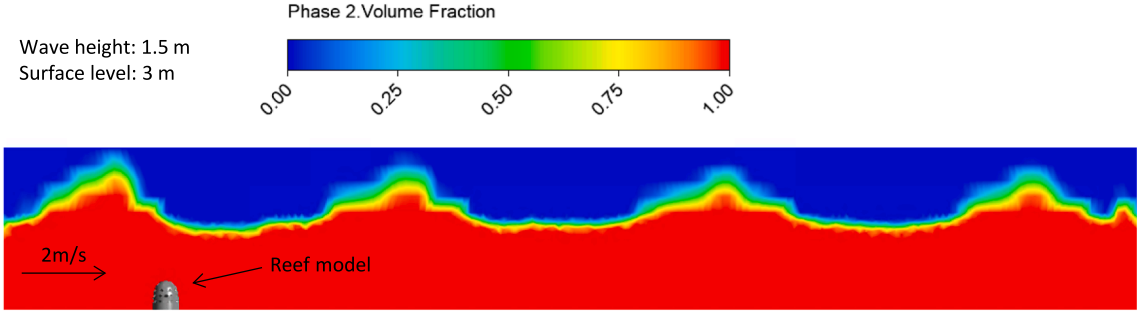

Fig. 8. Water volume fraction at a snapshot in time.

Table 3
Inventory sources.

Material/process	Source
Natural aggregates	[47–57]
Recycled aggregates	[58]
Fly ash	[59]
Nano-silica	[60]
Combustion of fossil fuel	[47]

Table 4
CML 2001 (January 2016 update) environmental categories.

Categories abbreviation	Categories name	Units
ADP elements	Abiotic Depletion (elements)	kg Sb eq.
ADP fossil	Abiotic Depletion (fossil)	MJ
AP	Acidification Potential	Kg SO2 eq.
EP	Eutrophication Potential	Kg Phosphate eq.
FAETP	Freshwater Aquatic Ecotoxicity Pot.	Kg DCB eq.
GWP	Global Warming Potential	Kg CO2 eq.
HTP	Human Toxicity Potential	Kg DCB eq.
MAETP	Marine Aquatic Ecotoxicity Pot.	Kg DCB eq.
ODP	Ozone Layer Depletion Potential	Kg R11 eq.
POCP	Photochemical Ozone Creation Potential	Kg Ethene eq.
TETP	Terrestrial Ecotoxicity Potential	Kg DCB eq.

Table 5
Weighting factors.

Impacts	Weighting
Abiotic Depletion (elements)	8
Abiotic Depletion (fossil)	7.7
Acidification Potential	6.3
Eutrophication Potential	8.7
Freshwater Aquatic Ecotoxicity Pot.	4.2
Global Warming Potential	27.8
Human Toxicity Potential	14.5
Marine Aquatic Ecotoxicity Pot.	4.8
Ozone Layer Depletion Potential	7.4
Photochemical Ozone Creation Potential	6.6
Terrestrial Ecotoxicity Potential	4

CML 2001 (January 2016 update) characterisation method was selected to calculate the potential environmental impacts produced by each of the mixtures since it is the one recommended by the standard EN 15804-2012 [54] for the development of Environmental Product Declaration of construction products. The impacts characteristics analysed by this method are shown in Table 4.

However, these environmental impacts where normalized and weighted to create a single score to feed the MCDM. Normalisation was made by dividing the impacts by the number of impacts produced in 2000 by the 28 European member states. Weighing was made by applying the values proposed by Lizasoain-Arteaga et al. [61] as an average of the weights proposed by the EPA, BEES NOGEPA and BREE (Table 5). More details on the LCA and inventory analysis used are developed in [37].

2.5. Multi-Criteria Decision-Making (MCDM)

MCDM was a useful tool employed to select the most promising mixtures among all the alternatives preselected. In this sense, the criteria considered were the material cost, environmental impact measured by application of the LCA, printability of the mix by the 3D printer and bio-receptivity. Although the compressive strength of the mixture was considered as another possible criteria, later it was discarded since it was considered more appropriate to normalise it in the materials cost and environmental impact criteria. In the same way, the bio-receptivity was parametrised by the amount of organic matter adhered to each mortar for the same surface (the average of 3 prismatic samples in the 4 countries). For the assignment of relative weights, a set of surveys were prepared and answered by fourteen members of the Technology and Construction Research Group (GITECO) and partners of the 3DPARE project which funded this investigation, being half of them engineers and the other half biologists. The questionnaire was prepared in such a way that the respondents had to assign a score between 0 and 100, with zero being the least important value and 100 being the most relevant criterion. All the participants have full knowledge of the project carried out and have actively participated in the calculation of each of the values contained in each criterion. However, to reduce the bias in the decision-making process the surveys were sent on condition of anonymity. In other words, although some participants know each other, their opinions for the assignment of weights remained anonymous.

The Evaluation Distance from Average Solution (EDAS) initially proposed by Ghorabaee et al [57] for inventory classification was chosen in this research for ranking the mixtures. The method employs an algorithm whose base is on computing the average solution (AV) to then determine the positive (PDA) and negative (NDA) distances from the average solution for each one of the alternatives. Accordingly, the best alternative is the one with the highest values of PDA and the lowest values of NDA. In this paper, the EDAS methodology is compared with the WASPAS and TOPSIS methodologies, which were developed and explained in the paper [37].

2.6. 3D printing process

For the elaboration of the ARs, a Delta 3D printer model “WASP 3MT” was used, which is based on EMS technology and allows the fabrication of structures layer by layer, with a maximum printing volume of 1 m in diameter and 1 m in height (Fig. 9). The printhead consists of a hopper, inside which there is an endless screw connected to a stepper motor, which allows the material to travel to the nozzle, which has a diameter of 20 mm. The printhead has a feed speed between 100 and 200 mm/s and the endless screw between 100 and 400 rpm.

The mortars used were prepared in a planetary mixer with a capacity of 30 l and three rotational speeds 142, 234 and 429 rpm. The following steps were implemented for the preparation: the materials were premixed dry for 15 s at low speed, then water was gradually added and mixing continued for 2 min, after which time the additive was added; then the speed was changed to medium, and the mortar was mixed for a further 2 min. The 3D printer is located in a warehouse were temperature and humidity values varied during the whole printing process from 15 °C to 24 °C and from 50 % to 75 %, respectively.

Manufacturing by layer-by-layer deposition 3D printing presents several challenges, including the ability of printing objects with a high angle of inclination (or overhangs) and with holes [17]. In this work, in addition to these challenges for 3D printing artificial reefs, other challenges were added, such as the need to be able to move the printed pieces without manipulating them directly and to generate a continuous chain of production and consumption of mortar. The need to move the pieces responds to the fact that the 3D printing equipment is fixed, so, in order to get the most out of it, once the pieces were printed, they had to be removed to start printing a new one; but because the mortars took a long time to harden, they could not be manipulated directly.

2.7. Artificial reefs shipping and deployment plan

As mentioned in the previous section, the fabrication process also took shipping and deployment into consideration. The sand filling used as a temporary scaffolding system to allow printing the holes and overhangs, was also thought to be used as a shipping material to guarantee that the ARs unit did not suffer any damage during transportation. This technique has the disadvantage of increasing the overall weight of

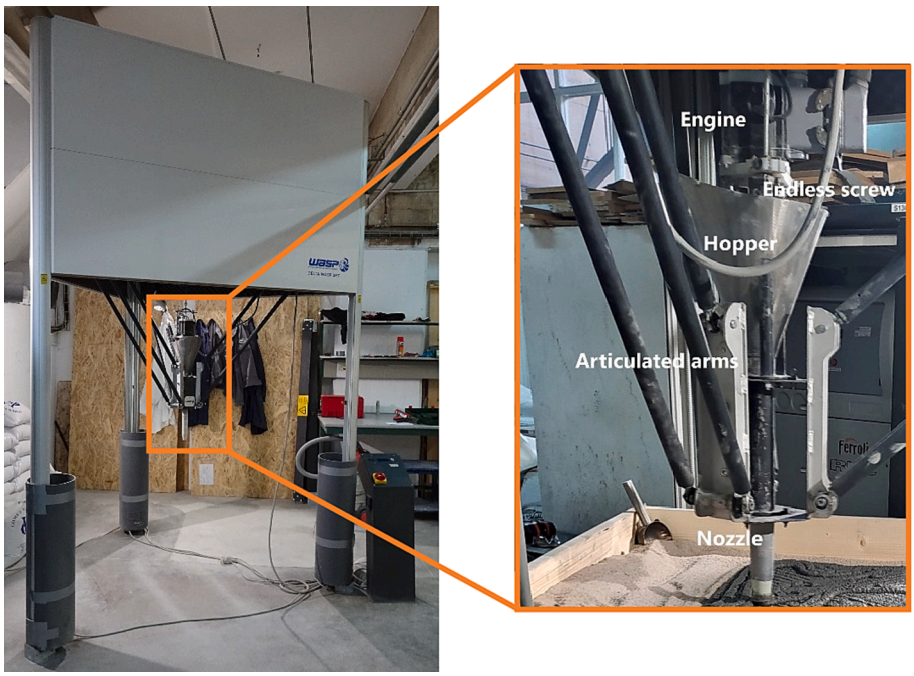

Fig. 9. 3D printer system details.

Fig. 10. Lifting plan.

each ARs unit, and therefore, increase the shipping cost slightly. However, the shipping costs are related not only with weight by also by volume. Therefore, the 9 ARs units might occupy, no matter their weight, a whole track.

In terms of deployment, it was considered that the most adequate system was to use 4 slings to be attached to the 4 eye bolts in the bottom steel plate. The design of each AR unit also considered that the slings should not break any overhang. Therefore, in the contact points of the sling with the ARs there were not overhangs (Fig. 10).

3. Results and discussion

3.1. Biomass, strength, printability and cost

Fig. 11 shows the results of the biomass according to the types of mortars analysed. No significant difference is observed between the cement and the geopolymer mortars for the same location, so that the higher or lower biological receptivity is more influenced by the maritime setting than by the type of mortar. However, analysing the average values, a higher amount of biomass is observed in the geopolymer specimens than in the cement specimens. A possible explanation of this finding is that there could be a positive role of NaOH in maximizing biomass productivity and CO_2 biofixation of a microalga as it has been also addressed by [62]. Also, another possible explanation is that depending on the concentration it could be that NaOH helps adsorption of toxic chemicals for marine organisms.

In a recent study on leaching and bioassays (inhibition of luminescence and sea urchin embryogenesis) carried out on mortars used for this research, it was concluded that cement mortars presented better leaching behaviour than geopolymer mortars, and that mortars with the use of marine shells presented low environmental acceptance, probably due to the degradation of the organic matter adhered to the shells [63]. These behaviours seem to be unrelated to the biomass results obtained in Fig. 11, but it should be taken into account that the specimens are exposed in a marine environment where a dissolution and removal effect of the leachates recorded can occur. In addition, both the pH and the composition of the hydrated products of the mortars could have an effect on the biomass recorded.

Although mortars immersed for longer periods (up to 24 months)

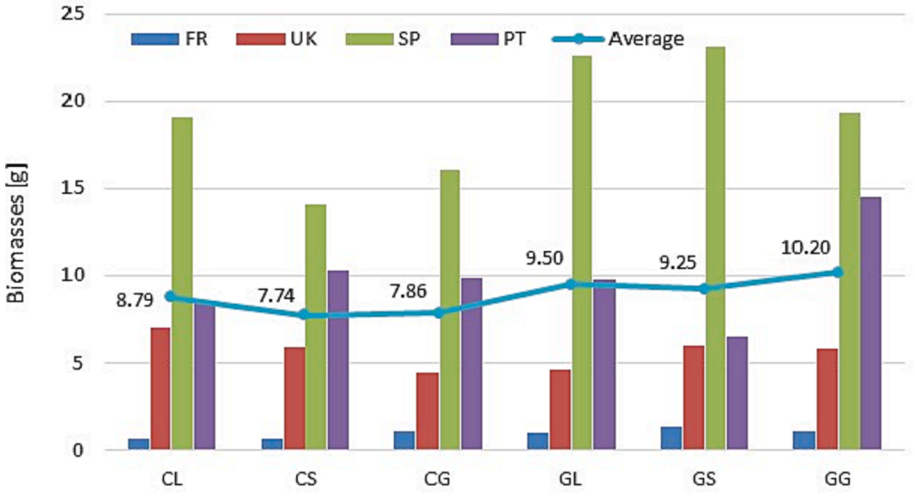

Fig. 11. Biomass content in the specimens for type of mortar after 3 months of immersion.

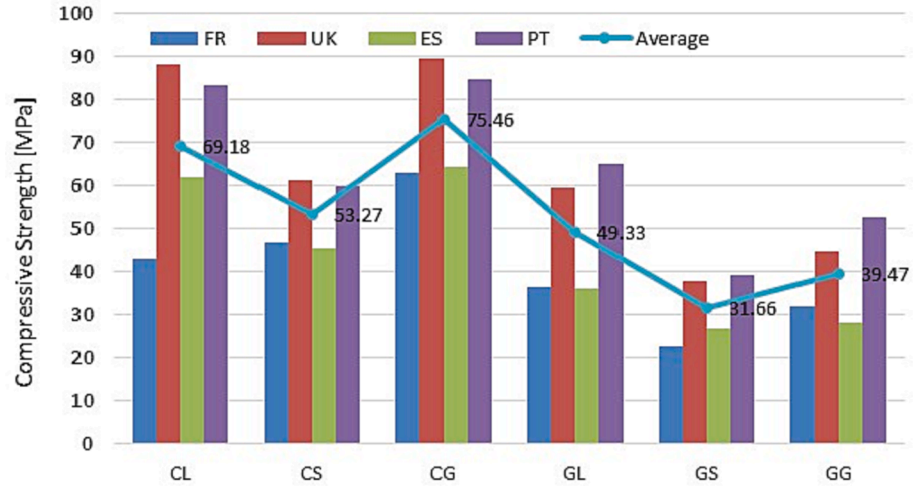

Fig. 12. Resistance to compression of mortars after 3 months of immersion in the sea.

resulted in higher and more variable biomass values [56], for the purposes of the MCDM analysis, biomass values for each type of material were considered after three months.

The compressive strength values show a large difference according to the type of material and according to the exposure site (Fig. 12). It is clearly observed that cement mortars show higher compressive strength values compared to geopolymer mortars; whereas, according to the exposure location of the specimens, a large dispersion in the results is observed. This dispersion can be attributed, on the one hand, to the heterogeneity of the specimens due to the 3D printing manufacturing that left small cavities between the extrusion filaments, and on the other hand, due to the marine exposure conditions of each country.

For the MCDM analysis, average compressive strength values were considered, not as specific criteria, but instead, to standardise the LCA and cost criteria, as it can be seen in Table 9.

Printability of cement mortars was quantified with a value of 3 (very good), while geopolymers were assessed with 2 (good) based on the scale proposed at [37]. Table 6 summarises the printability values of the 6 mortars.

The cost of the mortars normalised with density and compressive strength, which are used in the MCDM analysis, is shown in Fig. 13. The details of the cost analysis are given in the paper [37]. It is observed that the production cost associated to the geopolymer mortars is higher (around 6 times higher) than cement mortar, basically due to the high cost of NaOH and additives and penalised, in turn, by a lower compressive strength.

Table 6
Printability.

Alternatives/Criteria	Printability [1–3]
CL	3
CS	3
CG	3
GL	2
GS	2
GG	2

The LCA has been included in a different section (3.3) due to its extension. Nevertheless, this would be one of the 4 criteria (cost, printability, LCA and bioreceptivity) that will be used to carry out the MCDMA.

3.2. CFD and structural results

Fig. 14 presents the water velocity and pressure around one of the proposed ARs geometries. It is interesting to highlight that higher velocity values for both ARs are obtained in the water region close to the

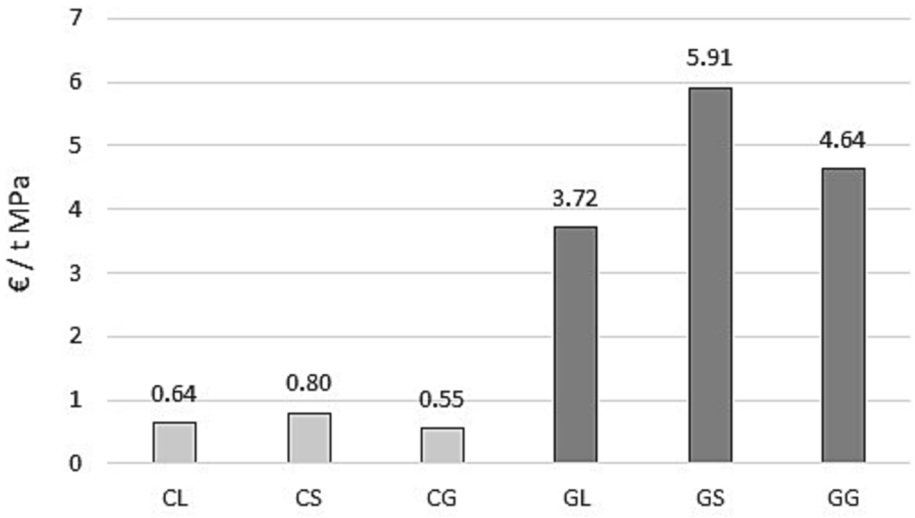

Fig. 13. Cost of parameterised materials.

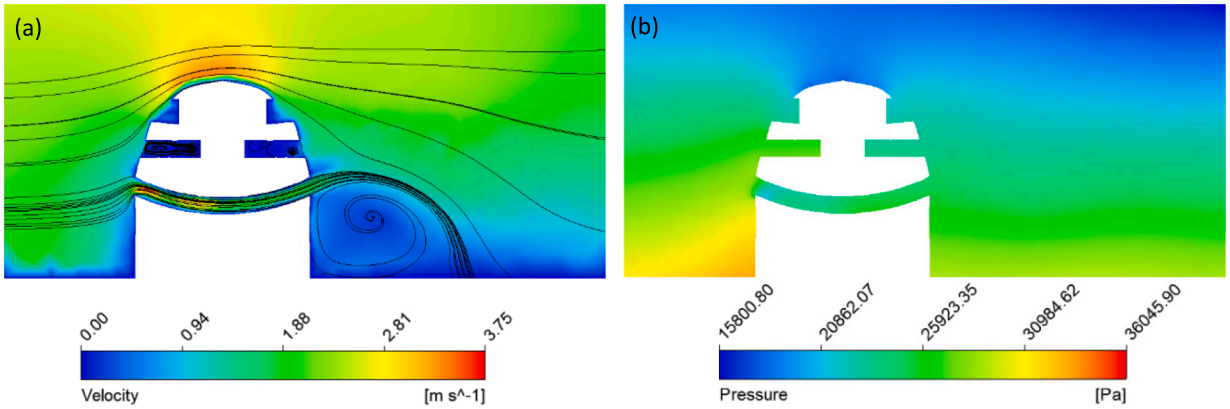

Fig. 14. Contour map of water velocity (a) and pressure (b) for the random artificial reef (random model).

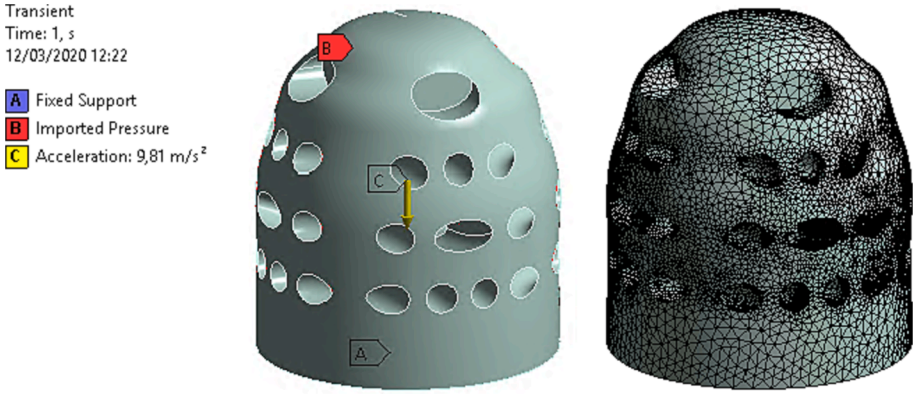

Fig. 15. Boundary condition defined in the structural analyses and the mesh built (random model).

top part of ARs and inside the channel that connects both sides of the ARs. In the ARs, the close cavities record lower velocity values; hence, these locations could be good places to harbour marine wildlife. The streamline enables to appreciate the vortices regions generated in the leeward side of reef. The water pressure is higher in the windward side of the ARs than the leeward side due to the direction of the prevailing water stream.

A transient structural analysis was carried out to evaluate the ARs stability under critical sea conditions. Therefore, the pressure acting on the ARs imported into the mechanical analyses was the one when the ARs records the maximum load values due to sea conditions. The boundary conditions set in the structural analyses are shown in Fig. 15. In the real conditions, the bottom surface of the ARs is not fixed to the sea surface; however, in the numerical simulation it was considered because this causes a higher value of drag force acting on the ARs. This is a conservative measure to analyse the stress recorded in the ARs.

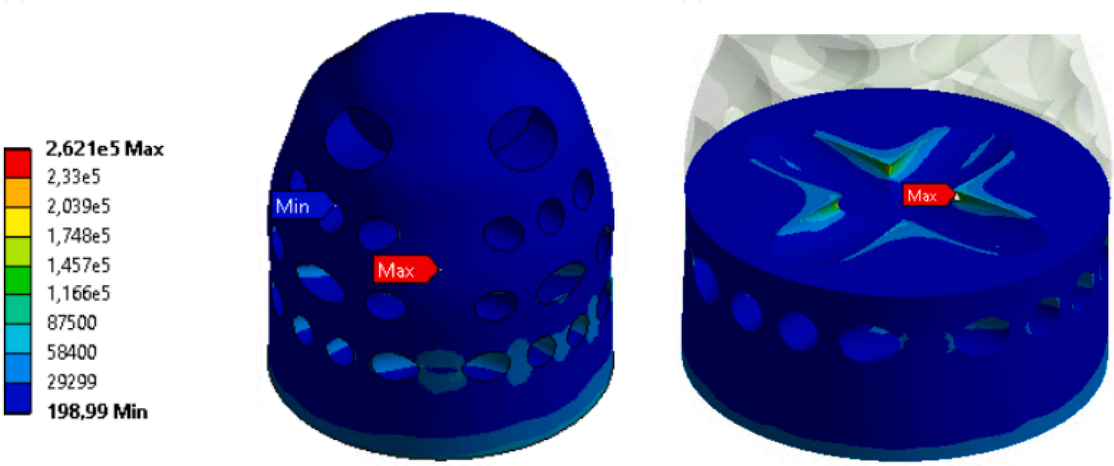

Fig. 16. Von Mises equivalent stress in the ARs (random model).

Fig. 16 shows the equivalent stress of Von Misses values recorded in one of the ARs geometries at the time when the critical forces were obtained. The random model ARs has a shape more similar to a sphere, which is advantageous for the stability of ARs since the drag force was significantly lower than in the cubic model. Consequently, this better aerodynamic behaviour is translated into slightly lower values of equivalent stress (Von Misses). The maximum value of equivalent stress is obtained in the arc of cavities, what could be caused when the water stream increases suddenly through the holes by the combined effect of waves and streams. Therefore, it is likely that the side surface of holes is working in tensile conditions and, consequently, this value must be compared against ultimate tensile stress of material. The ARs was built with materials whose minimum value of compressive strength was 39.2 MPa. This value was substituted in the next expression to obtain the ultimate tensile strength:

$$f_{ct,k} = 0.21 \bullet (f_{ck})^{2/3} \quad (1)$$

where $f_{ct,\ k}$ is the minimum tensile strength value and $f_{c\ k}$ is the compressive strength value.

The minimum tensile strength value of ARs material is 2.5 MPa from the Eq. (1), thus both ARs must withstand the sea force according to the structural analyses.

In addition, a motion analysis of ARs was carried out to evaluate if the ARs are moved or knocked over by the combined effect of waves and streams. The maximum drag force and lift force from CFD study were considered along with a friction coefficient of 0.4 between the ARs and sea floor to evaluate whether the ARs slides and knocks over. The results indicate that the ARs neither knocks over nor slides since the stabilising moment of 6979 N•m is much higher than the rollover moment of 543 N•m, and the friction force of 6979 N is significantly higher than the maximum drag force of 1628 N.

3.3. Life Cycle Assessment (LCA)

The LCA results achieved can be checked in Table 7 and Fig. 17. Results show that the environmental impact of the mixtures is highly related with their resistance; that is why cement-based mixtures perform better than geopolymers. Furthermore, CG and CL mixtures, having the highest compressive strengths produce the lowest environmental impact while GS, achieving the smallest resistance, produces the highest environmental impact.

3.4. Multi-Criteria Decision Making (MCDM)

The absolute frequencies and the cumulative relative histogram for the four criteria according to the respondents opinion are displayed in Fig. 18. Based on these data, descriptive statistics were carried out and the main results are described in Table 8. The normality distribution of the four criteria values (Table 9) was assessed according to the Anderson-darling test. The bio-receptivity criterion was the only normally distributed and with the highest weightage followed by the environmental impact, printability and materials cost. The U Mann-Whitney non-parametric test was done with confidence level of 95 % to find statistical differences among the criteria. Despite of the slight variations over the relative weights, no statistical differences were found between the bio-receptivity criterion in relation to printability and Environmental impact. However, with respect to materials cost criterion the difference was significant.

Fig. 19 shows the preference ranking for the six mixtures obtained by applying the EDAS method. The appraisal score for each alternative (AS_i) varies from zero to one as it can be observed. According to EDAS algorithm, the highest value of AS_i is the best alternative among all the alternatives selected whereas the alternative with the lowest value of AS_i

Table 7
Normalised and weighted environmental impacts.

Impact	Normalised and weighted environmental impacts					
	CL	CS	CG	GL	GS	GG
ADP elements	4.51E-15	5.65E-15	3.51E-15	6.04E-13	1.17E-12	7.94E-13
ADP fossil	1.29E-12	1.60E-12	1.08E-12	3.81E-12	6.54E-12	4.82E-12
AP	7.50E-13	9.46E-13	6.70E-13	1.62E-12	2.80E-12	2.06E-12
EP	1.43E-13	1.89E-13	1.31E-13	2.41E-13	4.36E-13	3.14E-13
FAETP inf.	3.56E-14	4.36E-14	3.10E-14	8.20E-14	1.36E-13	1.03E-13
GWP	6.67E-12	8.34E-12	5.88E-12	8.96E-12	1.51E-11	1.13E-11
HTP inf.	1.01E-11	1.28E-11	9.14E-12	3.36E-12	5.66E-12	4.27E-12
MAETP inf.	5.03E-12	5.95E-12	4.21E-12	1.67E-11	2.76E-11	2.08E-11
ODP	4.70E-18	7.66E-18	3.66E-18	2.16E-20	3.63E-20	2.70E-20
POCP	6.85E-13	8.87E-13	6.28E-13	1.17E-12	2.08E-12	1.52E-12
TETP inf.	8.51E-14	1.06E-13	7.56E-14	8.81E-14	1.46E-13	1.10E-13
TOTAL	2.47E-11	3.08E-11	2.18E-11	3.66E-11	6.17E-11	4.61E-11

Note: C: cement; G: geopolymer; L: limestone sand; S: shell sand; y G: glass sand.

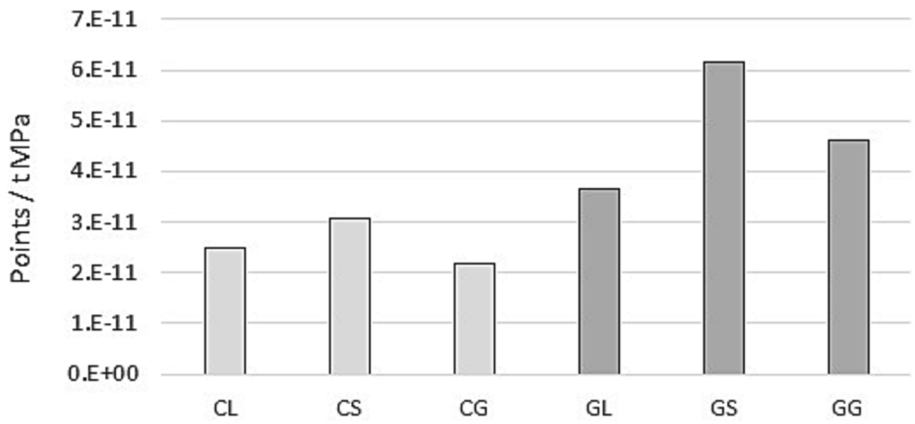

Fig. 17. Normalised and weighted environmental impacts.

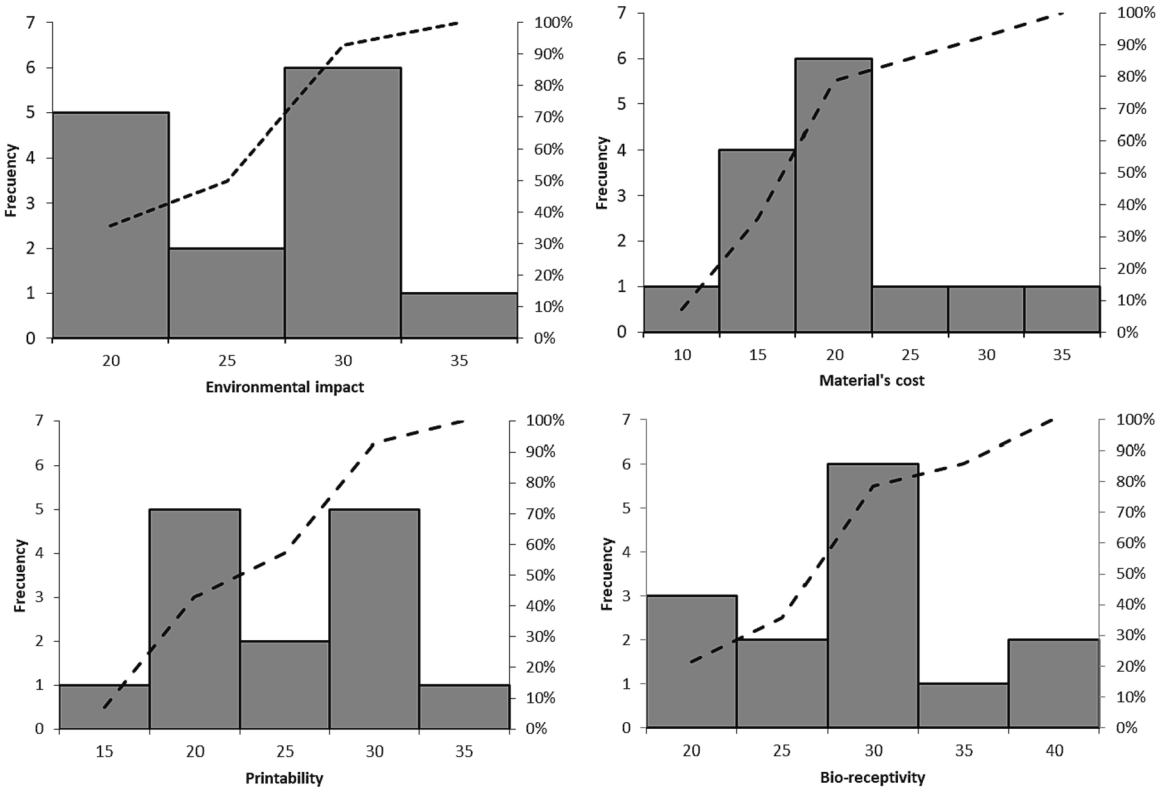

Fig. 18. Frequencies and cumulative relative histogram for the four criteria.

Table 8
Statistical parameters obtained from the questionnaires.

Statistical parameters	Environmental impact	Materials cost	Printability	Bio-receptivity
Mean	26.07	20.00	25.00	28.93
Median	27.50	20.00	25.00	30.00
Mode	30.00	20.00	30.00	30.00
Standard deviation	5.25	6.50	5.88	6.56
Coefficient of variation	0.20	0.33	0.24	0.23
Range	15.00	25.00	20.00	20.00
Min	20.00	10.00	15.00	20.00
Max	35.00	35.00	35.00	40.00
Normality (p – value)	<0.005	<0.006	<0.007	0.074

Table 9
Values of the four criteria.

Alternatives/ Criteria	Environmental impact	Materials cost	Printability	Bio-receptivity
	[Points LCA / t MPa]	[€ / t MPa]	[1–3]	[g]
CL	2.47E-11	0.64	3	8.79
CS	3.08E-11	0.80	3	7.74
CG	2.18E-11	0.55	3	7.86
GL	3.66E-11	3.72	2	9.50
GS	6.17E-11	5.91	2	9.25
GG	4.61E-11	4.64	2	10.20

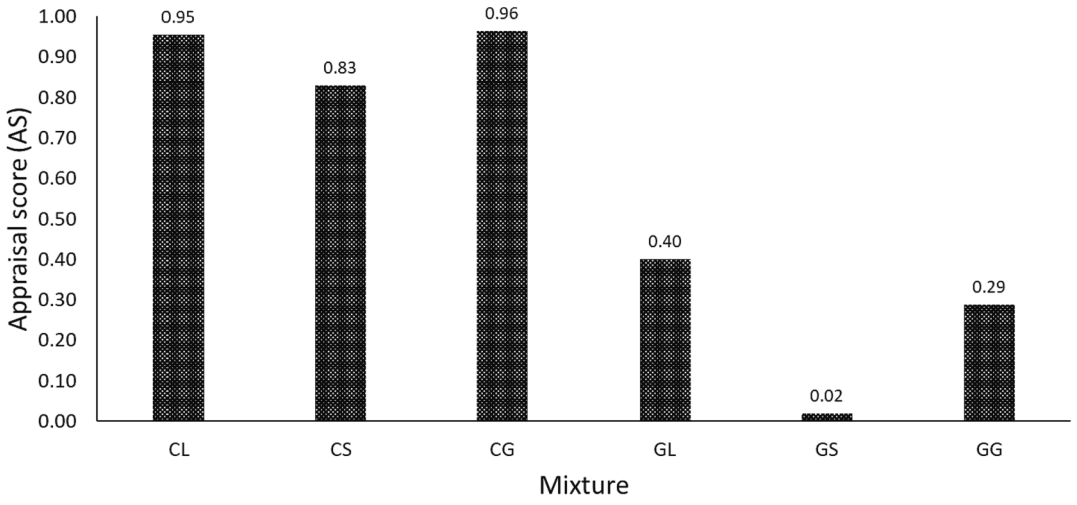

Fig. 19. Appraisal score obtained according to the EDAS method.

indicates the less preferred option. In that sense, mixtures manufactured with cement as binder were the most preferred options followed by geopolymer mixes. Although the CG alternative was ranked as the most suitable option, it should be emphasized that the *AS* of the CL alternative was also very close to the best and, hence, it could be considered as another possible mixture. Regarding the geopolymer mixes, despite having shown greater bio receptivity values when compared to cement mortars, they were ranked in the last positions. This was due to geopolymers presenting higher costs and environmental impact than cement mortar mixes. The explanation could be attributed to the sodium hydroxide used for manufacturing mortars and the use of additives, which are necessary to achieve conditions of printability and mechanical strength.

The results obtained by EDAS approach was also compared with other multi-criteria techniques to observe differences in the preference ranking obtained. To that end, technique for order preference by similarity solution (TOPSIS) and weighted aggregated sum product assessment (WASPAS) were the other two algorithms deemed to that purpose. Fig. 20a and Fig. 20b show the relationship between the closeness coefficient (CC) values and Joint performance Score (JPS) values calculated by TOPSIS and WASPAS techniques in relation to AS values. Although the main aim of this research is not to perform a comparison with other MCDM tools, it is advisable to carry them out as a checking process tool. Meanwhile, in the EDAS method the preference ranking of alternatives is based on the distance from the average solution. In the TOPSIS method, the best choice is determined according to the Euclidean distances from the positive and negative ideal solutions. On the other hand, the WASPAS approach is the product of the combination of other two tools denoted as weighted sum model (WSM) and weighted product model (WPM). In this research, a good correlation was found between EDAS approach with TOPSIS and WASPAS methods, respectively. In both cases, the preference ranking was the same with the performance values fitting inside the confidence interval lines and with R^2 values higher than 0.95.

3.5. 3D printing artificial reefs

With the results of biological receptivity, compressive strength, printability and cost, an MCDM analysis was carried out, which led to the conclusion that the two mortars with the best characteristics studied were CL and CG. These two mortars formed the two impression materials used to manufacture the artificial reefs.

As described previously, the 3D printing equipment used in this work has a simple head with a single nozzle, so in order to respond to the challenges presented, we proceeded as follows. To provide a solution to the continuous feeding of the printer, two planetary mixers (as described above) were used, working alternately or in parallel, depending on the demand for mortar. The mobility of the artificial reefs without direct manipulation was achieved by the use of pallets that functioned as temporary printing beds and were then moved with a hydraulic trolley.

A hybrid system of contour crafting and powder bedding was developed to print the holes and overhangs of the artificial reef models. The equipment was programmed to print only the contour of the ARs and as the number of layers increased, the areas corresponding to solid zones were filled with mortar and the areas corresponding to hollow zones were filled with sand (1–2 mm silica sand). The filler sand fulfilled two functions, the main one being to act as a printing base in the areas of overhangs and holes, and the secondary-one, to act as a support and confinement for the printed piece. As the sand alone cannot support itself, removable perimeter fences were installed as the printing progressed, and served to contain the sand (Fig. 21). Once the mortar had hardened, the perimeter fences and sand were removed. Both the fences and the sand could be reused in the printing of the subsequent ARs.

The 3D printing methodology implemented allowed the ARs to be printed in an average time of 6 h 45 min per piece. In addition, the digital models of the artificial reefs (Fig. 22) were successfully reproduced without settling or deformation during the printing process.

3.6. Artificial reefs shipping and deployment plan

The whole 36 ARs were built between October 2019 and February 2020 with an average production rate of 1 unit every 2 days (1 day for preparing all the materials, 1 day to build one unit). The 36 ARs were loaded (Fig. 23a) and shipped from Spain to UK in November 2019, to France in January 2020 and to Portugal in February 2020 and none of the units presented any damage when received (Fig. 23b). It can be concluded that the methodology of leaving the scaffolding sand also as a packaging protection filling material was adequate.

The 36 ARs were successfully immersed between March and June 2020 in the four locations: UK (17th March 2020), France (18th-19th May 2020), Spain (20th May 2020, see Fig. 24) and Portugal (3rd June 2020). Lockdowns due to the COVID 19 pandemic enforced a delay to immersion in France, Portugal and Spain. The UK managed to immerse the ARs right before their lockdown.

The lifting process using 4 slings attached to the steel plate was adequate and did not show any complexity. Also, as expected, it was necessary the use of professional scuba divers to assist the crane to locate in the right position each unit. Otherwise, especially in those locations

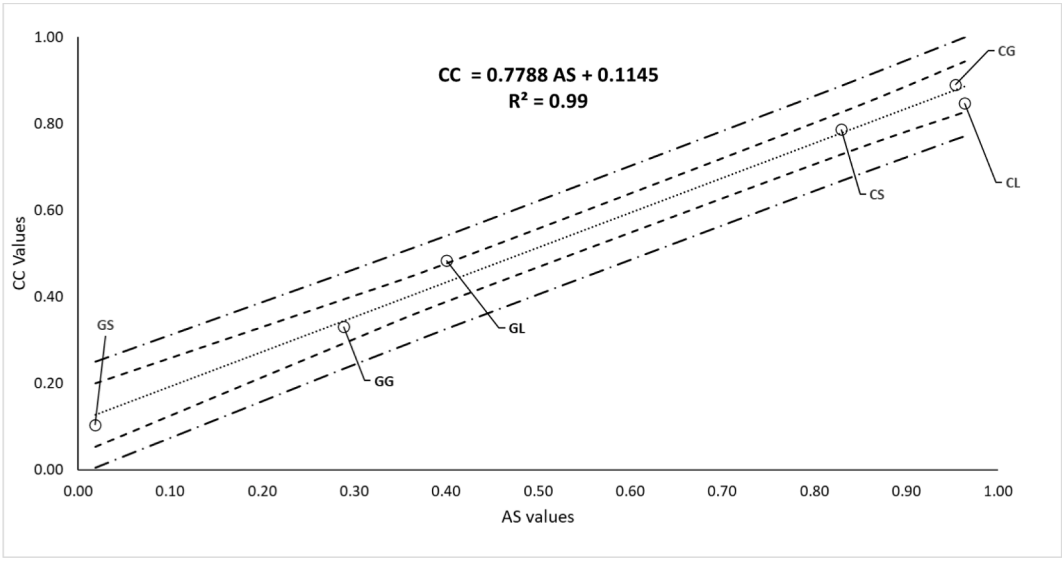

(a)

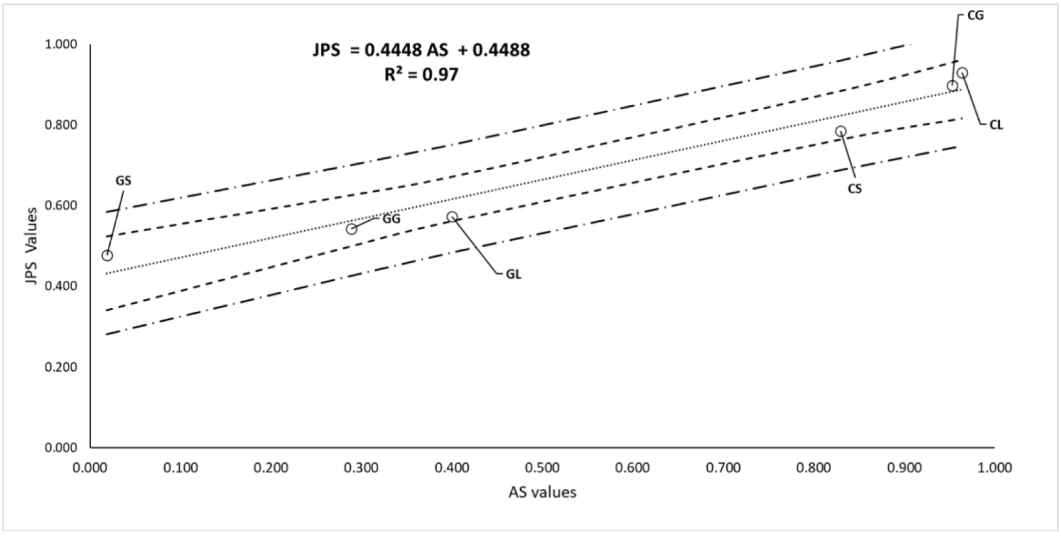

(b)

Fig. 20. Relationship observed between EDAS approach with respect to other MCDM methods. (a) TOPSIS; (b) WASPAS.

Fig. 21. Methodology for the production of ARs. Sequence of manufacturing progress.

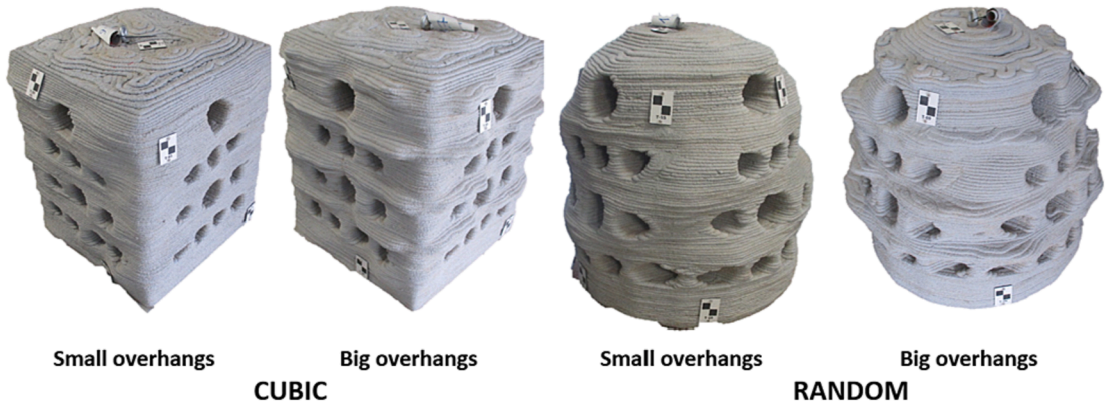

Fig. 22. The four-3D printed ARs models.

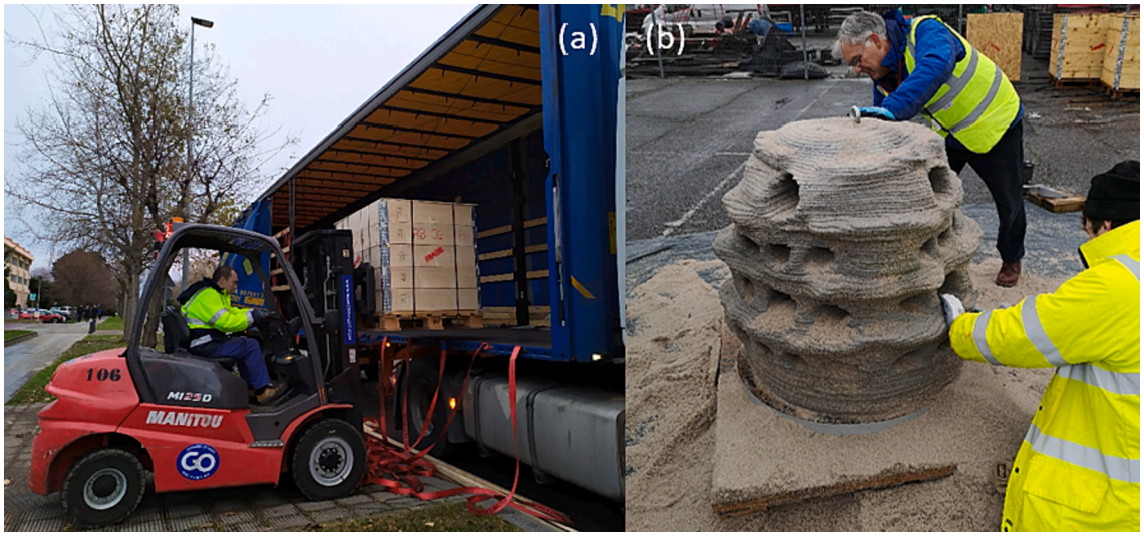

Fig. 23. Loading the crates into a truck at Santander (a), artificial reef unpacking at Poole Bay, UK (b).

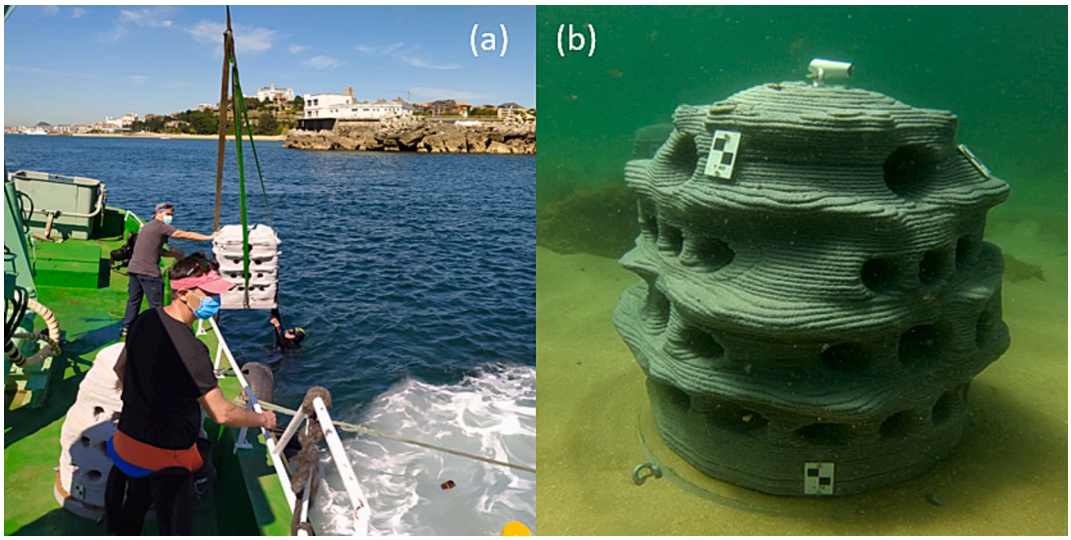

Fig. 24. Deployment from a vessel at Santander Bay (a), artificial reef after immersion (b).

that combined sandy and rocky bottom, an appropriate support on top of the sand could not be guaranteed just using a crane. For locations with just a flat sandy bottom, a vessel equipped with a crane without the use of scuba divers could be adequate, as long as very precise positioning of each reef unit is not required.

4. Conclusions

This work proposes the design of ARs to be 3D printed with the aim to create a most attractive habitat for both marine flora and fauna. In this sense, a numerical simulation was carried out of the conditions under which the ARs were going to be submitted, ensuring in this way their stability in the seabed, and different cement mortar and geopolymer mortar dosages were analysed to determine the mixture with the best properties for the fabrication of ARs. The conclusions extracted from the work done, are the following:

- The printability performance of both types of mortars is similar, independent of the type of aggregate used. The parameterised costs of geopolymer mixes are much higher than cement mortars, which is attributed to the use of NaOH and additives in high proportions.
- After three months of immersion in the sea, geopolymer mortars show higher biological receptivity compared to cement mortars. This is, on average, between 0.46 g and 2.46 g more biomass. The compressive strength is higher in the cement mortars, being, on average, between 3.94 MPa and 43.80 MPa higher than in the geopolymer mortars.
- Numerical simulation showed that the ARs designs exhibit structural integrity against marine loads and that they remain stable in their positions, without sliding or overturning.
- LCA showed that the mixtures with the highest compressive strength, CG and CL, produce the lowest environmental impact; while those with lowest strength, as GS, produce the highest environmental impact.
- According to the parameters analysed (cost of the mixtures, LCA, printability and biological receptivity), MCDM confirmed, objectively, that the mixtures with the best characteristics to be used in the manufacture of ARs by 3D printing are the CG and CL mixtures.
- The 3D printing methodology implemented for the manufacture of the ARs allowed the digital models to be faithfully reproduced. The challenges posed were solved satisfactorily. However, as the printing equipment did not have an automated feeding system, had a simple head with a single printing nozzle and was fixed to the floor, manpower was required to compensate for these limitations.
- The systematic approach used for the design of the ARs will allow us to find out in the future what types and sizes of holes, textures, shapes and overhangs are most attractive to marine life. The ARs have been survey for 2 years to obtain these results and monitorisation is planned to continue for one additional year.
- For large-scale projects that involve the production of many customised pieces but with similar shape among them, it might be useful to install a 3D printer in situ in the final deployment area to avoid shipping costs and energy consumption. Also, as an alternative, the production of a plastic mould through 3D printing with customised shapes might also be an interesting strategy when a complex shape is required to produce a reduced (but not unique) number of ARs.
- The use of mortars with low environmental impact for the production of ARs was sought. Thus, cement-based mortars with low clinker content and geopolymer-based mortars were analysed, as several authors point out that the production of geopolymers is more sustainable than that of cement-based materials [30,64–67].

CRediT authorship contribution statement

Adrian I. Yoris-Nobile: Conceptualization, Methodology, Investigation, Writing – original draft. **Carlos J. Slebi-Acevedo:** Conceptualization, Methodology, Investigation, Writing – original draft. **Esther Lizasoain-Arteaga:** Conceptualization, Methodology, Investigation, Writing – original draft. **Irune Indacoechea-Vega:** Conceptualization, Methodology, Investigation, Writing – original draft. **Elena Blanco-Fernandez:** Conceptualization, Methodology, Investigation, Writing – original draft. **Daniel Castro-Fresno:** Conceptualization, Methodology, Investigation, Writing – original draft. **Alejandro Alonso-Estebanez:** Conceptualization, Methodology, Investigation, Writing – original draft. **Sara Alonso-Cañon:** Conceptualization, Methodology, Investigation, Writing – original draft. **Carlos Real-Gutierrez:** Conceptualization, Methodology, Investigation, Writing – original draft. **Fouad Boukhelf:** Conceptualization, Writing – review & editing. **Mohamed Boutouil:** Conceptualization, Writing – review & editing. **Nassim Sebaibi:** Conceptualization, Writing – review & editing. **Alice Hall:** Conceptualization, Writing – review & editing. **Sam Greenhill:** Conceptualization, Writing – review & editing. **Roger Herbert:** Conceptualization, Writing – review & editing. **Richard Stafford:** Conceptualization, Writing – review & editing. **Bianca Reis:** Conceptualization, Writing – review & editing. **Pieter van der Linden:** Conceptualization, Writing – review & editing. **Oscar Babé Gómez:** Conceptualization, Writing – review & editing. **Hugo Sainz Meyer:** Conceptualization, Writing – review & editing. **João N. Franco:** Conceptualization, Writing – review & editing. **Emanuel Almada:** Conceptualization, Writing – review & editing. **Maria Teresa Borges:** Conceptualization, Writing – review & editing. **Isabel Sousa-Pinto:** Conceptualization, Writing – review & editing. **Miriam Tuaty-Guerra:** Conceptualization, Writing – review & editing. **Jorge Lobo-Arteaga:** Conceptualization, Writing – review & editing.

Declaration of Competing Interest

The authors declare that they have no known competing financial interests or personal relationships that could have appeared to influence the work reported in this paper.

Data availability

Data will be made available on request.

Acknowledgements

This work has been co-financed by the European Regional Development Fund through the Interreg Atlantic Area Programme, under the project *"Artificial Reef 3D Printing for Atlantic Area - 3DPARE"* (EAPA_174/2016). Besides, the authors want to thank the following companies for their contribution: Solvay, for supplying the fly ash and sodium hydroxide; BASF, for providing the additives used in the research; Abonomar S.L., for providing the seashells sand; FCC ámbito, for providing the crushed recycled glass and Grupo Cementos Portland Valderribas (Mataporquera plant) for providing the cement.

This work reflects the authorś opinion, so the authorities of the programme are not responsible for the use of the information here included.

References

[1] A. Becker, M.D. Taylor, H. Folpp, M.B. Lowry, Managing the development of artificial reef systems: the need for quantitative goals, Fish Fish. 19 (4) (2018) 740–752, https://doi.org/10.1111/faf.12288.
[2] M. Hammond, T. Bond, J. Prince, R.K. Hovey, D.L. McLean, An assessment of change to fish and benthic communities following installation of an artificial reef, Reg. Stud. Mar. Sci. 39 (2020), https://doi.org/10.1016/j.rsma.2020.101408.
[3] A.B. Paxton, K.W. Shertzer, N.M. Bacheler, G.T. Kellison, K.L. Riley, J.C. Taylor, Meta-analysis reveals artificial reefs can be effective tools for fish community enhancement but are not one-size-fits-all, Front. Mar. Sci. 7 (2020), https://doi.org/10.3389/fmars.2020.00282.
[4] J. Ramos, et al., An artificial reef at the edge of the deep: an interdisciplinary case study, Ocean Coast. Manag. 210 (2021), https://doi.org/10.1016/j.ocecoaman.2021.105729.

[5] J.S. Lima, P. Sanchez-Jerez, L.N. dos Santos, I.R. Zalmon, Could artificial reefs increase access to estuarine fishery resources? Insights from a long-term assessment, Estuar. Coast. Shelf Sci. 242 (2020), https://doi.org/10.1016/j.ecss.2020.106858.

[6] D. Cardenas-Rojas, E. Mendoza, M. Escudero, M. Verduzco-Zapata, Assessment of the performance of an artificial reef made of modular elements through small scale experiments, J. Mar. Sci. Eng. 9 (2) (2021) 1–18, https://doi.org/10.3390/jmse9020130.

[7] H. Pickering, D. Whitmarsh, A. Jensen, Artificial reefs as a tool to aid rehabilitation of coastal ecosystems: Investigating the potential, Mar. Pollut. Bull. 37 (8–12) (1999) 505–514, https://doi.org/10.1016/S0025-326X(98)00121-0.

[8] A. Tessier, et al., Assessment of French artificial reefs: due to limitations of research, trends may be misleading, Hydrobiologia 753 (1) (2015) pp, https://doi.org/10.1007/s10750-015-2213-5.

[9] H.R. Lemoine, A.B. Paxton, S.C. Anisfeld, R.C. Rosemond, C.H. Peterson, Selecting the optimal artificial reefs to achieve fish habitat enhancement goals, Biol. Conserv. 238 (2019), https://doi.org/10.1016/j.biocon.2019.108200.

[10] B. Vivier, et al., Marine artificial reefs, a meta-analysis of their design, objectives and effectiveness, Glob Ecol Conserv 27 (2021), https://doi.org/10.1016/j.gecco.2021.e01538.

[11] E. Riera, D. Lamy, C. Goulard, P. Francour, C. Hubas, Biofilm monitoring as a tool to assess the efficiency of artificial reefs as substrates: Toward 3D printed reefs, Ecol. Eng. 120 (2018) 230–237, https://doi.org/10.1016/j.ecoleng.2018.06.005.

[12] Q. Xu, T. Ji, Z. Yang, Y. Ye, Preliminary investigation of artificial reef concrete with sulphoaluminate cement, marine sand and sea water, Constr. Build. Mater. 211 (2019) 837–846, https://doi.org/10.1016/j.conbuildmat.2019.03.272.

[13] J. Sempere-Valverde, E. Ostalé-Valriberas, G.M. Farfán, F. Espinosa, Substratum type affects recruitment and development of marine assemblages over artificial substrata: a case study in the alboran sea, Estuar. Coast. Shelf Sci. 204 (2018) 56–65, https://doi.org/10.1016/j.ecss.2018.02.017.

[14] M. MacArthur, L.A. Naylor, J.D. Hansom, M.T. Burrows, Ecological enhancement of coastal engineering structures: passive enhancement techniques, Sci. Total Environ. 740 (2020), https://doi.org/10.1016/j.scitotenv.2020.139981.

[15] J.S. Mohammed, Applications of 3D printing technologies in oceanography, Methods Oceanogr. 17 (2016) 97–117, https://doi.org/10.1016/j.mio.2016.08.001.

[16] M. Trilsbeck, N. Gardner, A. Fabbri, M.H. Haeusler, Y. Zavoleas, M. Page, Meeting in the middle: hybrid clay three-dimensional fabrication processes for bio-reef structures, Int. J. Archit. Comput. 17 (2) (2019) 148–165, https://doi.org/10.1177/1478077119849655.

[17] R.A. Buswell, W.R. Leal de Silva, S.Z. Jones, J. Dirrenberger, 3D printing using concrete extrusion: a roadmap for research, Cem. Concr. Res. 112 (2018) 37–49, https://doi.org/10.1016/j.cemconres.2018.05.006.

[18] Crouse. M, "3D Printed Coral Reefs," *Design World*, 2016. https://www.designworldonline.com/3d-printed-coral-reefs/ (accessed Jul. 27, 2022).

[19] ReefDesignLab, "3D printed reefs. Large scale 3D printed oyster reef structures for the north sea," 2021. https://www.reefdesignlab.com/3d-printed-reefs-1. (accessed Jul. 27, 2022).

[20] R. Frost, "3D printing is helping to regenerate Hong Kong's precious coral reefs," *euronews.green*, 2021. Accessed: Jul. 27, 2022. [Online]. Available: https://www.euronews.com/green/2021/01/11/3d-printing-is-helping-to-rebuild-hong-kong-s-precious-coral-reefs.

[21] D. Klinges, "A new dimension to marine restoration: 3D printing coral reefs," *Mongabay*, 2018, Accessed: Jul. 27, 2022. [Online]. Available: https://news.mongabay.com/2018/08/a-new-dimension-to-marine-restoration-3d-printing-coral-reefs/.

[22] B. Reis, et al., Artificial reefs in the North –East Atlantic area: Present situation, knowledge gaps and future perspectives, Ocean Coast. Manag. 213 (2021), https://doi.org/10.1016/j.ocecoaman.2021.105854.

[23] B. Khoshnevis, Automated construction by contour crafting - Related robotics and information technologies, Autom. Constr. 13 (1) (2004) 5–19, https://doi.org/10.1016/j.autcon.2003.08.012.

[24] S. El-Sayegh, L. Romdhane, S. Manjikian, "A critical review of 3D printing in construction: benefits, challenges, and risks", Arch. Civ. Mech. Eng. 20 (2) (2020) https://doi.org/10.1007/s43452-020-00038-w.

[25] R.J.M. Wolfs, A.S.J. Suiker, Structural failure during extrusion-based 3D printing processes, Int. J. Adv. Manuf. Technol. 104 (1–4) (2019) 565–584, https://doi.org/10.1007/s00170-019-03844-6.

[26] X. Huang, Z. Wang, Y. Liu, W. Hu, W. Ni, On the use of blast furnace slag and steel slag in the preparation of green artificial reef concrete, Constr. Build. Mater. 112 (2016) 241–246, https://doi.org/10.1016/j.conbuildmat.2016.02.088.

[27] Y. Bigdeli, M. Barbato, C.D. Lofton, M.T. Gutierrez-Wing, K.A. Rusch, Mechanical properties and performance under laboratory and field conditions of a lightweight fluorogypsum-based blend for economic artificial-reef construction, J. Mater. Civ. Eng. 32 (7) (2020) pp, https://doi.org/10.1061/(ASCE)MT.1943-5533.0003240.

[28] EConcrete, "EConcrete," 2022. https://econcretetech.com/ (accessed Oct. 18, 2022).

[29] P. Duxson, J.L. Provis, G.C. Lukey, J.S.J. van Deventer, The role of inorganic polymer technology in the development of 'green concrete', Cem. Concr. Res. 37 (12) (Dec. 2007) 1590–1597, https://doi.org/10.1016/j.cemconres.2007.08.018.

[30] S.H. Teh, T. Wiedmann, A. Castel, J. De Burgh, Hybrid life cycle assessment of greenhouse gas emissions from cement, concrete and geopolymer concrete in australia, J. Clean. Prod. 152 (2017) 312–320, https://doi.org/10.1016/j.jclepro.2017.03.122.

[31] D.A. Salas, A.D. Ramirez, N. Ulloa, H. Baykara, A.J. Boero, Life cycle assessment of geopolymer concrete, Constr. Build. Mater. 190 (2018) 170–177, https://doi.org/10.1016/j.conbuildmat.2018.09.123.

[32] A. Passuello, et al., Evaluation of the potential improvement in the environmental footprint of geopolymers using waste-derived activators, J. Clean. Prod. 166 (Nov. 2017) 680–689, https://doi.org/10.1016/j.jclepro.2017.08.007.

[33] R. Bajpai, K. Choudhary, A. Srivastava, K.S. Sangwan, M. Singh, Environmental impact assessment of fly ash and silica fume based geopolymer concrete, J. Clean. Prod. 254 (May 2020), 120147, https://doi.org/10.1016/j.jclepro.2020.120147.

[34] T. Xie, T. Ozbakkaloglu, Behavior of low-calcium fly and bottom ash-based geopolymer concrete cured at ambient temperature, Ceram. Int. 41 (4) (2015) 5945–5958, https://doi.org/10.1016/j.ceramint.2015.01.031.

[35] R. Rodríguez-Álvaro, "Morteros para revestimiento con árido procedente de concha de mejillón," Universidade da Coruña, 2014. Accessed: Jul. 27, 2022. [Online]. Available: https://ruc.udc.es/dspace/handle/2183/13632.

[36] C. Martínez García, "Estudio del comportamiento de la concha de mejillón como árido para la fabricación de hormigones en masa: aplicación en la cimentación de un módulo experimental (Módulo Biovalvo)," Universidade da Coruña, 2016. Accessed: Jul. 27, 2022. [Online]. Available: https://ruc.udc.es/dspace/handle/2183/17489.

[37] A.I. Yoris-Nobile, et al., Life cycle assessment (LCA) and multi-criteria decision-making (MCDM) analysis to determine the performance of 3D printed cement mortars and geopolymers, J. Sustain Cem. Based Mater. (2022), https://doi.org/10.1080/21650373.2022.2099479.

[38] CEN- European Committee for Standardization, *EN 196-1:2016. Methods of testing cement. Part 1: Determination of strength*. 2016.

[39] O. Ly, et al., Optimisation of 3D printed concrete for artificial reefs: Biofouling and mechanical analysis, Constr. Build. Mater. 272 (2021), https://doi.org/10.1016/j.conbuildmat.2020.121649.

[40] S. Alonso-Cañon, E. Blanco-Fernandez, D. Castro-Fresno, A.I. Yoris-Nobile, L. Castanon-Jano, "Reinforcements in 3D printing concrete structures: a review,", Arch. Civ. Mech. Eng. (2022). In press.

[41] S. Pope, *Turbulent Flows*. Cambridge University Press, 2000.

[42] J. Tu, G. H. Yeoh, and C. Liu, *Computational Fluid Dynamics: a practical approach*, vol. Second. 2012.

[43] B. Andersson, et al., Computational Fluid Dynamics for Engineers, Cambridge University Press, New York, 2012.

[44] International Organization for Standardization, *ISO 14040: Environmental Management - Life Cycle Assessment - Principles and Framework, 2 nd*. 2006.

[45] International Organization for Standardization, *ISO 14044: Environmental Management - Life Cycle Assessment - Requirements and Guidelines, 1 edn*. 2006.

[46] E.R. Grist, K.A. Paine, A. Heath, J. Norman, H. Pinder, The environmental credentials of hydraulic lime-pozzolan concretes, J. Clean. Prod. 93 (2015) 26–37, https://doi.org/10.1016/j.jclepro.2015.01.047.

[47] NREL, "U.S. Life Cycle Inventory Database," 2012.

[48] A. Jullien, C. Proust, T. Martaud, E. Rayssac, C. Ropert, Variability in the environmental impacts of aggregate production, Resour. Conserv. Recycl. 62 (2012) 1–13, https://doi.org/10.1016/j.resconrec.2012.02.002.

[49] UNPG, "Module d'informations environnementales de la production de granulats issus de roches massives," 2011.

[50] UNPG, "Module d'informations environnementales de la production de granulats issus de roches meubles," 2011.

[51] H. Stripple, "Life Cycle Assessment of Road. A Pilot Study for Inventory Analysis," 2001. Accessed: Jul. 27, 2022. [Online]. Available: https://www.ivl.se/download/18.694ca0617a1de98f473458/1628416184474/FULLTEXT01.pdf.

[52] U. M. Mroueh, P. Eskola, J. Laine-Ylijoki, K. Wellman, E. Mäkelä, and M. Juvankoski, "Life cycle assessment of road construction," 2000.

[53] RE-ROAD, "Life Cycle Assessment of Reclaimed Asphalt," 2012.

[54] Y. Huang, "Life Cycle Assessment of Use of Recycled Materials in Asphalt Pavements," 2007.

[55] T. Häkkinen, K. Mäkelä, Environmental adaption of concrete. Environmental impact of concrete and asphalt pavements, VTT Tied. - Valt. Tek. Tutkimusk. no. 1752 (1996).

[56] Athena, "Cement and Structural Concrete Oroducts: Life Cycle Inventory Update #2," 2005.

[57] M. L. Marceau, M. Nisbet, and M. G. Vangeem, "Life Cycle Inventory of Portland Cement Concrete," 2011.

[58] UNPG, "Module d'informations environnementales de la production de granulats recyclés," 2011.

[59] L.K. Turner, F.G. Collins, Carbon dioxide equivalent (CO_2-e) emissions: a comparison between geopolymer and OPC cement concrete, Constr. Build. Mater. 43 (2013) 125–130, https://doi.org/10.1016/j.conbuildmat.2013.01.023.

[60] M. Yekkalar, M. R. Sabour, and M. Nikravan, "The environmental impacts of concrete containing Nano-SiO<inf>2</inf> and typical concrete on global warming and fossil fuel depletion: A comparison," in *Life-Cycle and Sustainability of Civil Infrastructure Systems - Proceedings of the 3rd International Symposium on Life-Cycle Civil Engineering, IALCCE 2012*, 2012, pp. 2435–2442.

[61] E. Lizasoain-Arteaga, I. Indacoechea-Vega, P. Pascual-Muñoz, D. Castro-Fresno, Environmental impact assessment of induction-healed asphalt mixtures, J. Clean. Prod. 208 (2019) 1546–1556, https://doi.org/10.1016/j.jclepro.2018.10.223.

[62] M. Nayak, S.S. Rath, M. Thirunavoukkarasu, P.K. Panda, B.K. Mishra, R. C. Mohanty, Maximizing biomass productivity and CO2 biofixation of microalga, scenedesmus sp. By using sodium hydroxide, J. Microbiol. Biotechnol. 23 (9) (2013) 1260–1268, https://doi.org/10.4014/jmb.1302.02044.

[63] J. Santos, et al., Assessment of the environmental acceptability of potential artificial reef materials using two ecotoxicity tests: Luminescent bacteria and sea

urchin embryogenesis, Chemosphere (2022), https://doi.org/10.1016/j.chemosphere.2022.136773.
[64] R. Bajpai, K. Choudhary, A. Srivastava, K.S. Sangwan, M. Singh, Environmental impact assessment of fly ash and silica fume based geopolymer concrete, J. Clean. Prod. 254 (2020), 120147, https://doi.org/10.1016/j.jclepro.2020.120147.
[65] A. Passuello, et al., Evaluation of the potential improvement in the environmental footprint of geopolymers using waste-derived activators, J. Clean. Prod. 166 (2017) 680–689, https://doi.org/10.1016/j.jclepro.2017.08.007.
[66] D.A. Salas, A.D. Ramirez, N. Ulloa, H. Baykara, A.J. Boero, Life cycle assessment of geopolymer concrete, Constr. Build. Mater. 190 (2018) 170–177, https://doi.org/10.1016/j.conbuildmat.2018.09.123.
[67] P. Duxson, J.L. Provis, G.C. Lukey, J.S.J. van Deventer, The role of inorganic polymer technology in the development of 'green concrete', Cem. Concr. Res. 37 (12) (2007) 1590–1597, https://doi.org/10.1016/j.cemconres.2007.08.018.